Journal of Superconductivity and Novel Magnetism (2021) 34:211–225
https://doi.org/10.1007/s10948-020-05677-x

ORIGINAL PAPER

Structural, Electronic, Magnetic, Elastic, Thermodynamic, and Thermoelectric Properties of the Half-Heusler RhFeX (with X = Ge, Sn) Compounds

M. A. Bennani[1] · Z. Aziz[1] · S. Terkhi[1] · E. H. Elandaloussi[2] · B. Bouadjemi[1] · D. Chenine[1] · M. Benidris[1] · O. Youb[1] · S. Bentata[3]

Received: 19 October 2019 / Accepted: 5 September 2020 / Published online: 17 September 2020

Abstract
In the present work, the structural, electronic, magnetic, elastic, thermodynamic, and thermoelectric properties of half-Heusler alloys RhFeX (with X = Ge, Sn) have been investigated using the full-potential linearized augmented plane wave (FP-LAPW) method based on density functional theory (DFT) implemented in the WIEN2k code. The generalized gradient approximation of Perdew-Burke-Ernzerhof (GGA-PBE) and the Tran-Blaha-modified Becke-Johnson exchange potential method (TB-mBJ) has been used for modeling exchange correlation potential. The results obtained show that the two studied compounds are mechanically and dynamically stable. On the other hand, both compounds RhFeX (with X = Ge, Sn) exhibit a half-metallic ferromagnet behavior; their magnetic moments obey the Slater-Pauling rule with an absolute bias of 100% around the Fermi level. The thermodynamic properties including the isothermal bulk modulus, the heat capacity, the Debye temperature, and the thermal expansion coefficients of both compounds are investigated using the quasi-harmonic Debye model. According to the thermoelectric results, the values of the merit factor (ZT) are 0.935 and 0.952 at 300 K for RhFeGe and RhFeSn, respectively; these results indicate that our compounds are potentially good candidates for thermoelectric applications at low temperature.

Keywords Half-Heusler · Density functional theory · Half-metallicity · Ferromagnetic · Thermodynamic and thermoelectric properties

1 Introduction

Half-metallic ferromagnet (HMF) compound is a new class of materials that has attracted a lot of attention because of their diverse applications. This notion is derived from their electronic structure, which exhibits a typically metallic behavior for one of the spin densities while the other one is semiconductor. The 100% spin polarization at the Fermi level (E_F) is one of the most exceptional properties for this class of materials. The half-metallicity property has been discovered for the first time within the half-Heusler alloy NiMnSb using first-principles calculations [1]. Recently, much attention has been attracted to study half-Heusler alloys [2, 3] and more specifically HMF for their interesting properties in such as magnetoelectronics and spintronics [4]. They also remain attractive for other technical applications such as spin injection devices [5], spin filters [6], tunnel junctions [7], or giant magnetoresistance devices [8, 9] due to high Curie temperature [10], and they are also promising candidates for environmentally friendly and inexpensive thermoelectric materials [11]. To date, the study of half-Heusler alloys has focused on their electronic and magnetic properties, but the thermodynamic and thermoelectric properties have not been treated at the same degree.

The objective of this study is to determine the structural, electronic, magnetic, elastic, thermodynamic, and thermoelectric properties of the two compounds RhFeX (with X = Ge, Sn) by firstly performing the generalized gradient

✉ Z. Aziz
zoubir.aziz@univ-mosta.dz

[1] Laboratory of Technology and Solid's Properties, Faculty of Sciences and Technology, Abdelhamid Ibn Badis University, BP 227, 27000 Mostaganem, Algeria

[2] The University Center of Relizane, Bourmadia, 48000 Relizane, Algeria

[3] Mustapha Stambouli University of Mascara, BP 305, 29000 Mascara, Algeria

approximation proposed by Perdew-Burke-Ernzerhof (GGA-PBE) [8, 12], while the electronic and magnetic properties are calculated using both the GGA-PBE approximation and the Tran-Blaha-modified Becke-Johnson (TB-mBJ) potential [13].

Debye's quasi-harmonic model is applied for studying the thermodynamic properties of our two compounds RhFeX (with X = Ge, Sn). Several thermodynamic quantities such as the Debye temperature θ_D, the bulk modulus B, the thermal capacity C_V, and the thermal expansion (α) could be calculated. Through the description of the computation model based on Boltzmann's semiclassical theory using the BoltzTraP code, the results of the electrical conductivity, the electronic thermal conductivity, the Seebeck coefficient, and the figure of merit are presented.

2 Calculation Method

The calculations in this work were carried out using full potential linearized augmented plane wave (FP-LAPW) method [4] implemented in the WIEN2k [14] code. The exchange-correlation energy is parameterized by the generalized gradient approximation proposed by Perdew-Burke-Ernzerhof (GGA-PBE) [8, 12]. DFT calculations, within the GGA-PBE scheme, are used to determine and obtain different properties of the compounds. For the study of electronic and magnetic properties, in addition to GGA-PBE, the approach called approximation of Becke-Johnson's modified potential by Tran and Blaha (TB-mBJ) was also used to achieve quite accurate band gaps due to comparison. In all studied configurations, non-magnetic, antiferromagnetic, and ferromagnetic, the $R_{MT}{\cdot}K_{max}$ parameter is taken equal to 8 where R_{MT} is the smallest muffin-tin radius and K_{max} is the maximum modulus of reciprocal vector in the first Brillouin zone, and the expansion of wave functions has been set to $l_{max} = 10$ within the muffin-tin. $G_{max} = 14$ where G_{max} is defined as the magnitude of the largest vector in the charge density Fourier expansion. The integration of the Brillouin area is carried out with 120 k-points based on a mesh size of 15 × 15 × 15 equivalent to 3400 k-points. The self-consistent calculations stop when the energy convergence reaches to 10^{-5}Ry. The WIEN2k code allows the calculation of three independent elastic constants C_{11}, C_{12}, and C_{44} for cubic systems by computing energy of crystal versus volume changes and applying different tetragonal and rhombohedral stress and strain. The other elastic parameters, such as modulus of elasticity and shear modulus, elastic anisotropy, and Poison ratio, can also be obtained from these independent constants. The Gibbs program was used to calculate the thermodynamic parameters, which is based on Debye's quasi-harmonic model [15, 16]; this method derives from the thermal equation of state (EOS) and appropriate standard thermodynamic relationships. The semiclassical Boltzmann theory [17, 18], as implemented in the BoltzTraP code, has been used to study thermoelectric properties. The relaxation time was maintained constant for the computation of the transport properties.

3 Results and Discussions

3.1 Structural Properties

This part is devoted to study the structural properties of our compounds RhFeX (with X = Ge, Sn). This kind of study is of major interest because it allows collecting information about the microscopic structure of materials and therefore has a relatively large impact on the prediction of other properties such as electronic, elastic, and thermal.

The half-Heusler alloys have the general formula XYZ and crystallize in a non-centrosymmetric cubic structure (space group number 216, F-43m, C_1b) [19]. This type of half-Heusler structure can be characterized by the interpenetration of three cubic face-centered sub-networks (cfc), which is occupied by the atoms X, Y, and Z (Fig. 1) [20]. The X and Y atoms considered without the Z atoms would form a zincblende structure. Similarly, the X and Z atoms considered without the Y atoms would also form a zincblende structure. In principle, three non-equivalent atomic arrangements are possible in this type of structure as summarized in Table 1. To obtain the equilibrium lattice constant and determine the stable structure of studied half-Heusler alloys, we perform structural optimizations on the RhFeGe and RhFeSn alloys for ferromagnetic (FM), antiferromagnetic (AFM), and non-magnetic (NM) phases for three configurations (1, 2, and 3) and are illustrated in Figs. 2a–c and 3a–c. The values of total energy as a function of volume are adjusted by the Birch-Murnaghan EOS [21]. The performed calculations were able to predict the ferromagnetic (FM) state of the three atomic configurations for the RhFeGe compound as well as for the RhFeSn alloy in the both configurations 1 and 3 but not in the configuration 2 where it is antiferromagnetic. From these three types of structures (1, 2, and 3) for the two compounds RhFeGe and RhFeSn, it is clear that the optimization has shown that the lowest energy is in the type 1 (see Fig. 1), and therefore, it can be concluded that this arrangement is the most stable for these two compounds (see Fig. 4a, b). Our optimized results for the lattice parameter a_0 (Å), bulk modulus B (GPa), and its first derivative B' calculated for the three possible atomic arrangements are presented in Table 2. The obtained lattice parameters for both compounds are in good agreement with those found by Jianhua Ma et al. [22]. In order to determine the thermodynamic stability and estimate the possibility of synthesizing RhFeX (with X = Ge, Sn) alloys, the formation enthalpy and the cohesive energy

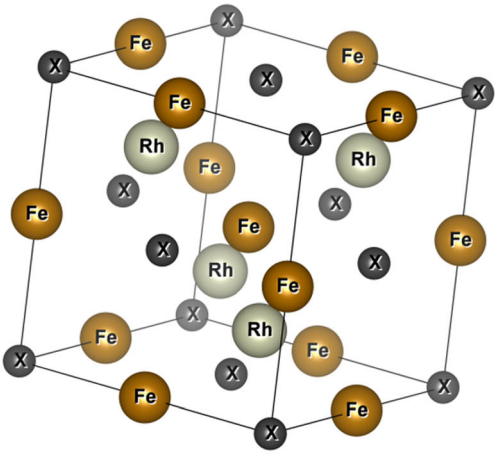

Fig. 1 Crystal structure of half-Heusler RhFeX (with X = Ge, Sn) (structure type (1))

were calculated. The formation energy of a crystal (ΔH_f^{xyz}) is defined as the difference between the energy of the crystal and the sum of the energies of the elements that make up this crystal in their standard states. (A body is said to be in the standard state when it is pure, unmixed, and in its most stable physical state.) The formation energy is computed using the following relationship:

$$\Delta H_f^{xyz} = E\frac{xyz}{\text{total}} - \left(E\frac{x}{\text{bulk}} + E\frac{y}{\text{bulk}} + E\frac{z}{\text{bulk}}\right) \quad (1)$$

where $E\frac{xyz}{\text{total}}$ is the total energy of the compound present in phase C_1b, and $E\frac{x}{\text{bulk}}$, $E\frac{y}{\text{bulk}}$, and $E\frac{z}{\text{bulk}}$ are the total energies calculated (per atom at $T = 0$ K) of the atoms in their standard states. The formation energy values for the two alloys studied are shown in Table 3. We can see that the formation energies calculated from Eq. (1) have negative values, which confirm the stability and the possibility to synthesize easily these compounds experimentally. Our results are in perfect agreement with those found in [23].

The cohesive energy of a compound XYZ is defined by the difference between the total primitive cell energy calculated at the equilibrium lattice constant $E\frac{xyz}{\text{total}}$ and the atomic energy calculated for the fundamental state configuration of X, Y, and Z according to the following equation:

$$E_{\text{coh}} = E_{\text{total}}^{xyz} - \left(E_{\text{atom}}^{x} + E_{\text{atom}}^{y} + E_{\text{atom}}^{y}\right) \quad (2)$$

Table 1 Inequivalent site occupancies within the C_1b-type structure for RhFeGe and RhFeSn

	X	*Y*	*Z*
Type 1	(1/4, 1/4, 1/4)	(1/2, 1/2, 1/2)	(0, 0, 0)
Type 2	(1/2, 1/2, 1/2)	(0, 0, 0)	(1/4, 1/4, 1/4)
Type 3	(0, 0, 0)	(1/4, 1/4, 1/4)	(1/2, 1/2, 1/2)

The cohesive energies obtained for RhFeGe and RhFeSn calculated using the GGA-PBE approximation are given in Table 2. The computed values in most stable physical state are negative for both compounds, which confirm the stability of the half-Heusler alloys RhFeX (with X = Ge, Sn).

3.2 Electronic Properties

The electronic properties, band structure and state density, depend essentially on the distribution of electrons in the valence and conduction bands, as well as on the value of the gap. These properties are calculated for half-Heusler ternary alloys RhFeX (with X = Ge, Sn) in their equilibrium state with the optimized lattice parameter of the most stable type 1 structure.

The spin-up and spin-down polarized band structures for the two compounds RhFeX (with X = Ge, Sn) with GGA-PBE and TB-mBJ approximations are calculated and presented in Fig. 5 (a1–a4, b1–b4). It is noteworthy that the majority spin band structures have metal intersections around the Fermi level for both RhFeGe and RhFeSn compounds, which indicates the pure metallic character of these electronic structures, while the minority spin structures of RhFeGe and RhFeSn exhibit semiconductor behavior, where the maximum of the valence band is located at point L for both approximations GGA-PBE and TB-mBJ and the minimum of the conduction band is located at point X for GGA-PBE and point W for TB-mBJ meaning the presence of an indirect gap in the directions (L-X and L-W) for GGA-PBE and TB-mBJ, respectively, for both compounds RhFeX (with X = Ge, Sn). It can be concluded that these different electronic behaviors between majority and minority spins lead to classify these compounds as half-metals. Our calculated band gap (E_g) of RhFeGe and RhFeSn based on the GGA-PBE approximation is in good agreement with the work reported in [23]. The different values of the physical properties of RhFeX (with X = Ge, Sn), such as gap energy (E_g) and half-metallic energy gap (E_{HM}), and

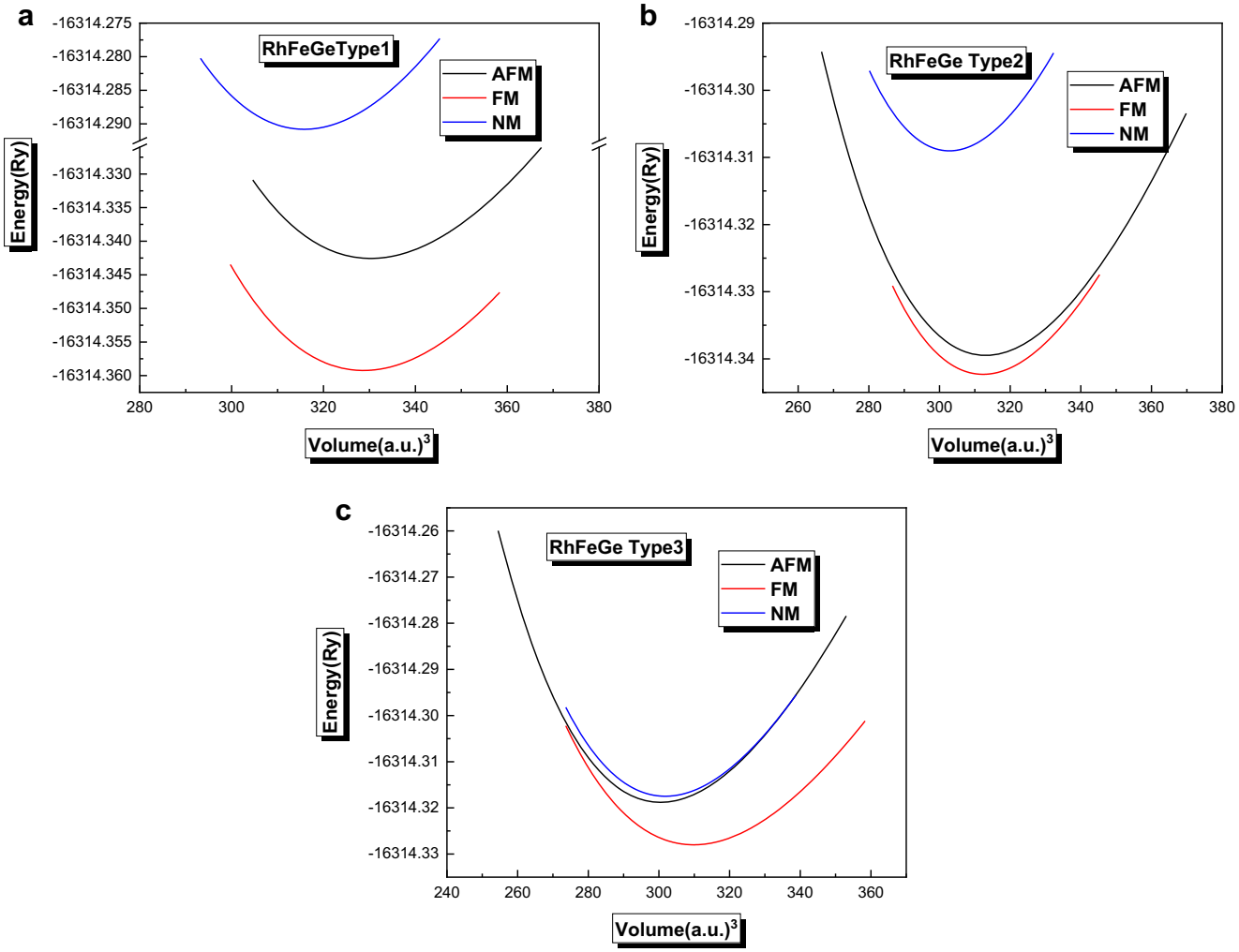

Fig. 2 Total energy as a function of volume for RhFeGe in type 1 (**a**), type 2 (**b**), and type 3 (**c**) for ferromagnetic and non-magnetic and antiferromagnetic states

Table 2 Calculated lattice a_0 (*A*), cohesive energy E_{coh} (Ry), bulk modulus *B* (GPa), and its first derivative *B′* in three possible atomic arrangements for RhFeGe and RhFeSn

Type	Method	Configuration	a_0 (A)		*B* (GPa)		*B′*		E_{coh} (Ry)	
			RhFeGe	RhFeSn	RhFeGe	RhFeSn	RhFeGe	RhFeSn	RhFeGe	RhFeSn
Type 1	GGA	FM	5.797	6.057	151.2	130.5	4.90	5.17	− 1.151	− 1.076
		NM	5.720	5.989	168.3	147.2	4.24	5.00	− 1.479	− 1.367
		AFM	-	-	145.1	125.1	5.28	5.13	− 1.175	− 1.075
Type 2		FM	5.699	6.067	154.1	114.6	5.18	5.22	− 1.134	− 0.996
		NM	5.640	5.999	178.4	138.2	4.80	4.85	− 1.498	− 1.321
		AFM	-	-	141.7	116.4	4.75	4.87	− 1.172	− 1.012
Type 3		FM	5.684	5.964	139.3	123.8	5.06	4.96	− 1.119	− 1.045
		NM	5.634	5.894	178.1	154.6	4.83	5.22	− 1.506	− 1.390
		AFM	-	-	177.3	123.2	4.90	4.51	− 1.151	− 1.056
	Other cal.		5.780[a]	6.050[a]	-	-	-	-	-	

[a] Ref [22]

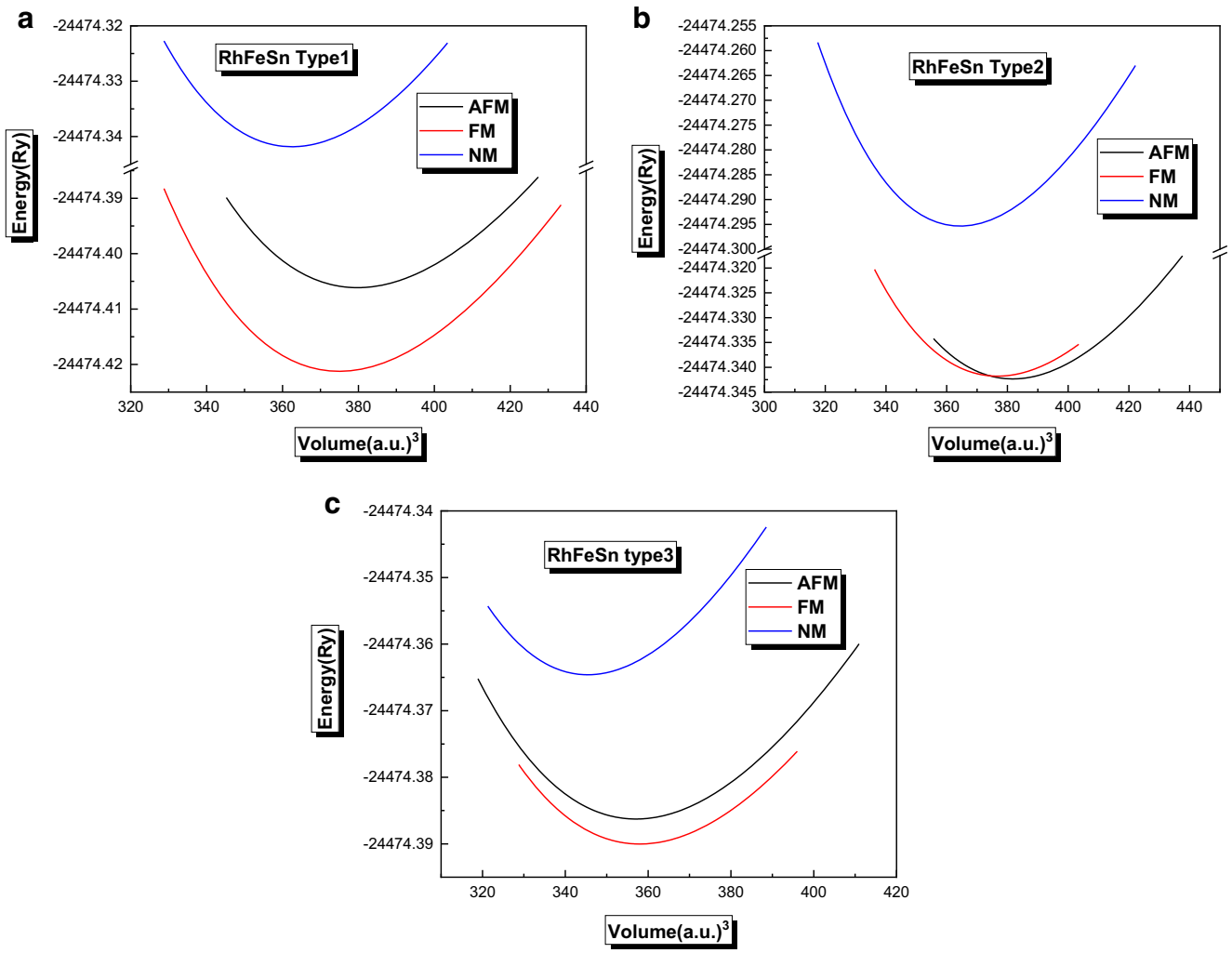

Fig. 3 Total energy as a function of volume for RhFeSn in type 1 (**a**), type 2 (**b**), and type 3 (**c**) for ferromagnetic and non-magnetic and antiferromagnetic states

physical nature of the material and tape transition calculated with GGA-PBE and TB-mBJ are given in Table 4. We can see that the E_g is more improved by TB-mBJ and then GGA-PBE, because the latter one underestimated the E_g [23], whereas the

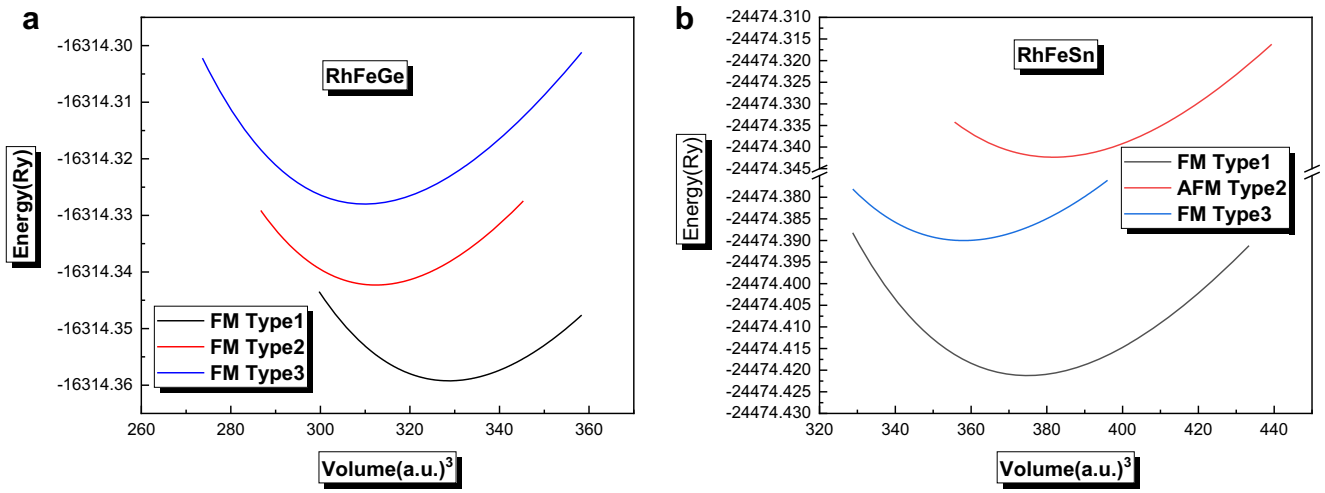

Fig. 4 Total energy as a function of volume in the three atomic arrangements type (1), type (2), and type (3) of RhFeGe (**a**) and RhFeSn (**b**) compounds

Table 3 Calculated formation energy ΔH_f (Ry) of RhFeGe and RhFeSn

Compound	ΔH_f (Ry)	
	This work	Other cal.
RhFeGe	− 0.106	− 0.139[a]
RhFeSn	− 0.085	− 0.121[a]

[a] Ref [22]

TB-mBJ approximation gives an accurate band gap close to the experimental one, as shown by many previous studies [24–27]. Furthermore, Table 4 presents also the calculated half-metallic gap energies. The half-metallic gap energy (E_{HM}) is defined as the minimum energy between the lowest energy of up-(down)-spin conduction bands with respect to Fermi level and the absolute values of the highest energy of the up-(down)-spin valence bands [28, 29]. The E_{HM} is 0.115 and 0.193 eV using GGA-PBE and 0.269 and 0.126 eV using TB-mBJ for RhFeGe and RhFeSn, respectively.

For understanding the band structures origin of the both materials, we have calculated the total density of states (TDOS) and partial density of states (PDOS) of the half-Heusler compounds RhFeX (with X = Ge, Sn) at their equilibrium lattice constant using the GGA-PBE and TB-mBJ approximations.

The states $5s^1 4d^8$ for Rh, $4s^2 3d^6$ for Fe, $4s^2 3d^{10} 4p^2$ for Ge, and $5s^2 4d^{10} 5p^2$ for Sn are treated as valence electrons. The TDOS and PDOS are computed and presented in Fig. 6 (a1–a4, b1–b4). The vertical line in red indicates the Fermi level (E_F).

In order to describe the electronic structures in detail, the d orbitals of transition metal Rh and Fe degenerated into double e_g (d_{z2} and d_{x2+y2}) state and triple t_{2g} (d_{xy}, d_{yz}, and d_{xz}) state are traced in PDOS. The DOS results are almost similar for both approximations with some difference in the gap width and in peaks position. At the Fermi level (E_F), in the spin up channel, it is clearly seen that the TDOSs of the both cubic half-Heusler RhFeX (with X = Ge, Sn) exhibit a conductor behavior. This character is mainly due to the contribution of d-eg and d-t2g orbitals of Rh and Fe atoms and weak one of p orbitals of Ge and Sn atoms. In contrast, the spin down channel forms band gap energy around the Fermi level which leads to a 100% spin polarization for GGA-PBE and TB-mBJ methods.

Below the Fermi level, in the valence bands, it is clear that there are two distinct regions in both spin cases. The first region between − 10.7 eV and − 8.55 eV for RhFeGe and − 9.7 eV and − 7.24 eV for RhFeSn is an isolated region of the others; it is mainly due to Ge 4s and Sn 5s orbitals and minor contribution of Rh d-t2g states. The second energy region between − 5.67 eV and − 0.44 eV for RhFeGe and − 4.98 eV and − 0.19 eV for RhFeSn is predominated by the Rh d-eg, Fe d-t2g, and weak contribution of the Ge 4p and Sn 5p state electrons.

Above the Fermi level, in the conduction bands, we can see that these regions are principally due to Fe d-t2g states and weak contribution of Rh d-t2g, Ge 4p, and Sn 5p orbitals.

3.3 Magnetic Properties

The magnetic moment is a very important factor when studying the magnetic properties of a material. It gives information about the rate of the magnetic field that the material has or the elements that constitute it. The behavior of the magnetic moments of spins in RhFeX (with X = Ge, Sn) compounds is studied. In Table 5 are listed the total and partial magnetic moments calculated with polarized spin in the muffin-tin spheres and in the interstitial sites using GGA-PBE and TB-mBJ approximations. The total magnetic moment (μ_{tot}) per cell unit is close to an integer Bohr magneton 3 μB for both materials, which confirms the half-metallic nature of these two compounds. Our results for the magnetic moments of RhFeGe and RhFeSn are in perfect agreement with the obtained values by Jianhua Ma et al. [22]. From Table 5, the values obtained illustrate that the magnetic moment of each compound is mainly contributed by the transition metal Fe with low contributions of Rh, Ge, and Sn atoms. In addition, the opposite values of the atomic magnetic moments of Fe atom with Ge and Sn atoms for RhFeGe and RhFeSn alloys clearly indicate that the valence band contains the Ge 4p and Sn 5p states interacting in opposite ways with the Fe 3d states. Galanakis et al. [30] have shown that in the case of half-metallic Heusler

Table 4 Calculated energy gap E_g (eV), half metallic energy gap E_{HM} (eV), band gap transition, and physical state for RhFeGe and RhFeSn

Material	Method	E_g (eV)		E_{HM}	Band transition	Physical state
		This work	Other cal.			
RhFeGe	GGA	0.484	0.49[a]	0.115	L → X	HM
	TB-mBJ	0.850	-	0.269	L → W	HM
RhFeSn	GGA	0.482	0.48[a]	0.193	L → X	HM
	TB-mBJ	0.758	-	0.126	L → W	HM

[a] Ref [22]

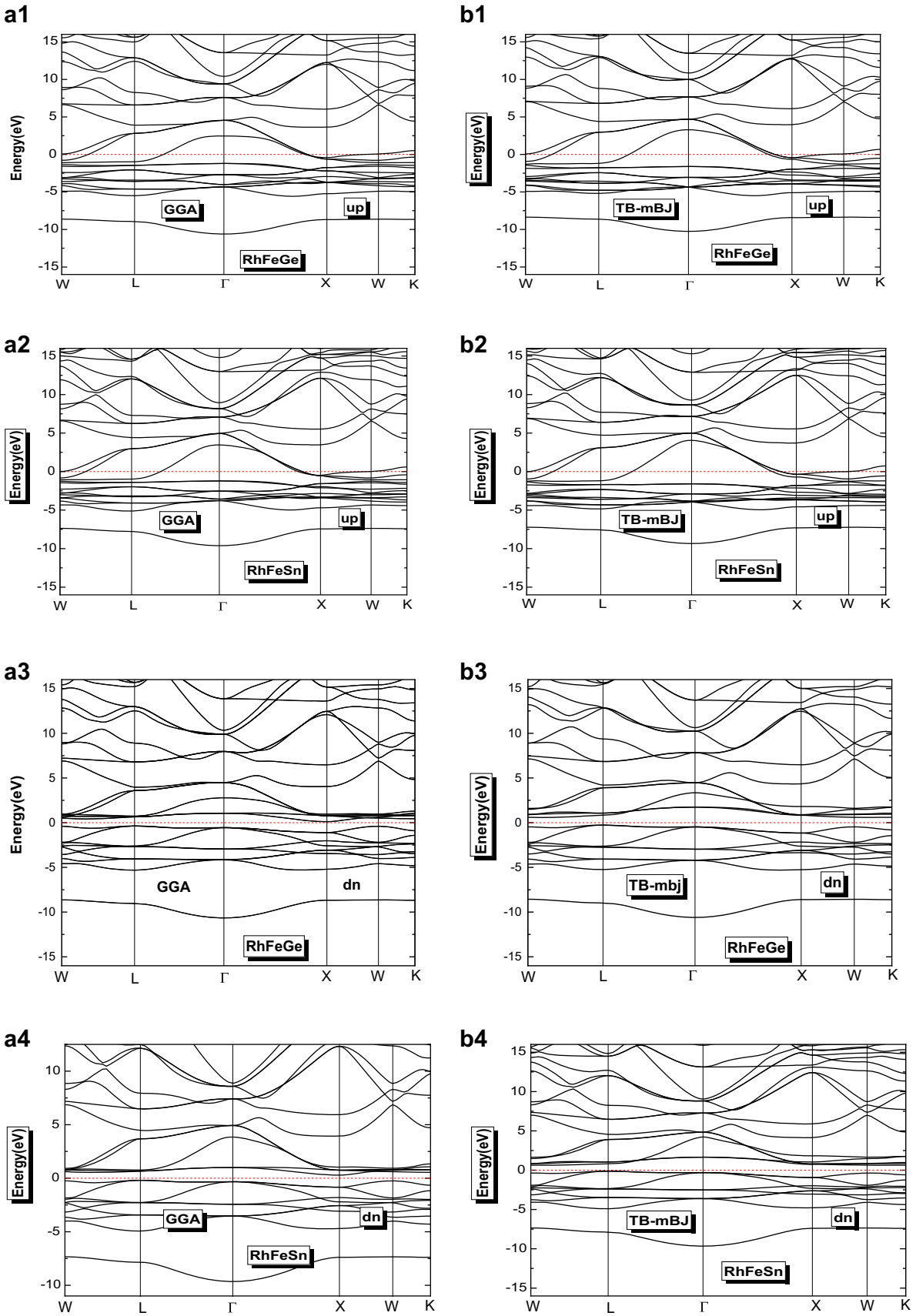

Fig. 5 Spin up and spin down band structure of RhFeGe and RhFeSn using (a1–a4) GGA and (b1–b4) TB-mBJ

alloys, the total magnetic moment follows a well-defined relationship called the Slater-Pauling rule: $\mu_{tot} = (Z_{tot} - 18)$, where Z_{tot} is the total number of valence electrons, even for compounds containing less than 24 electrons such as the alloys studied in our work. The total number of valence electrons for RhFeGe and RhFeSn is 21; thus, we find that the total magnetic moment is integer the value equal to 3 μB, which confirms that our two compounds have a half-metallic character.

3.4 Elastic Properties

Materials with cubic crystal structure have three independent elastic constants: C_{11}, C_{12}, and C_{44}. All results for elastic

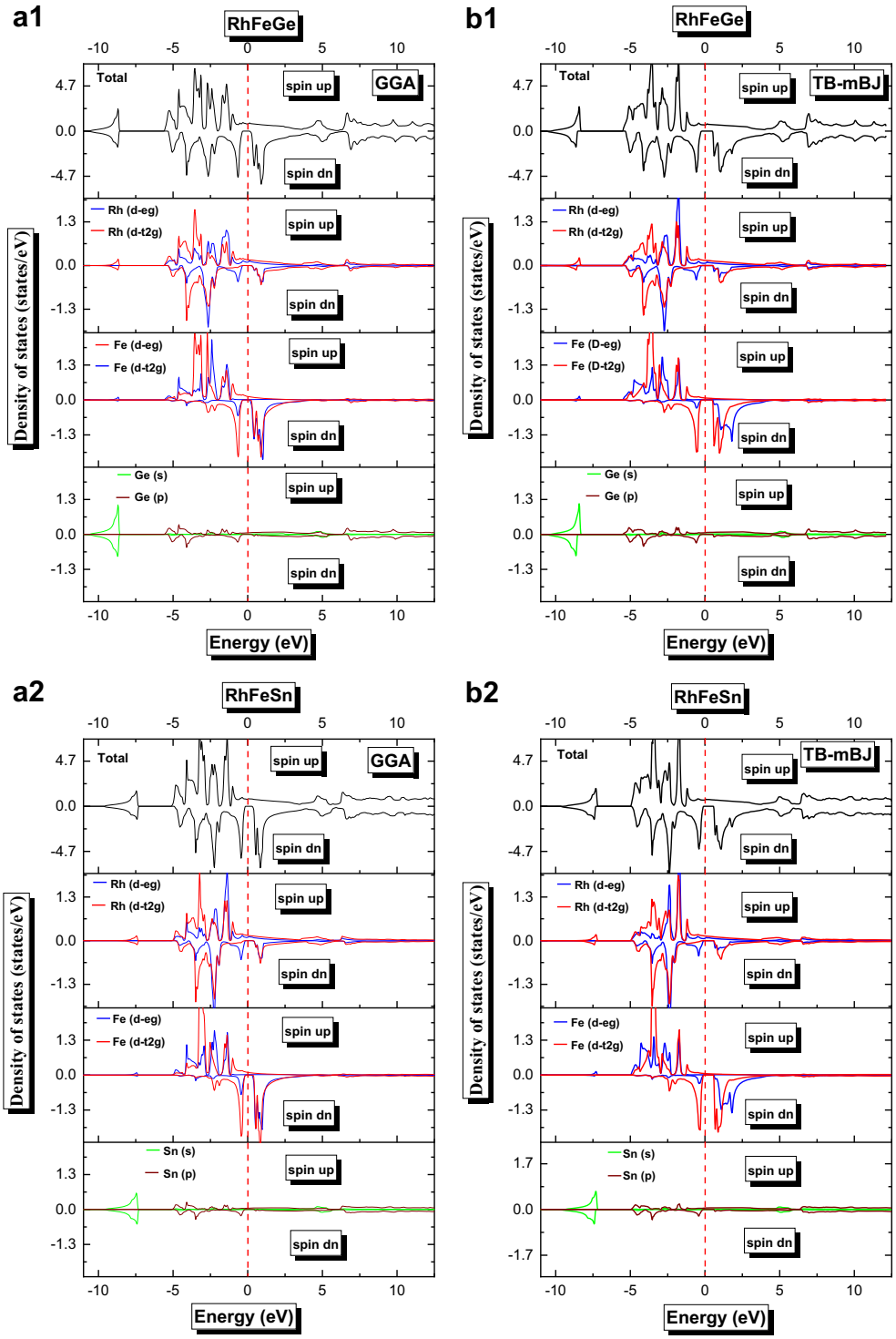

Fig. 6 The calculated total and partial density of states of cubic RhFeGe and RhFeSn using (a1–a4) GGA and (b1–b4) TB-mBJ

Table 5 Calculated total and partial magnetic moments (in Bohr magneton, μB) for RhFeGe and RhFeSn compounds with GGA and TB-mBJ approximations

	RhFeGe				RhFeSn		
	GGA		TB-mBJ		GGA		TB-mBJ
	Other cal.	This work			Other cal.	This work	
μ^{Rh}	0.201[a]	0.24	0.25	μ^{Rh}	0.192[a]	0.23	0.25
μ^{Fe}	2.908[a]	2.90	3.10	μ^{Fe}	2.978[a]	2.98	3.15
μ^{Ge}	− 0.102[a]	− 0.06	− 0.11	μ^{Sn}	− 0.094[a]	− 0.05	− 0.08
$\mu^{interstitial}$	-	− 0.08	− 0.24	$\mu^{interstitial}$	-	− 0.12	− 0.32
μ^{Total}	3.00[a]	3.00	3.00	μ^{Total}	3.00[a]	3.04	3.00

[a] Ref [22]

constants (C_{11}, C_{12}, and C_{44}), Young modulus E, shear modulus G, Poisson's coefficient υ, anisotropy parameter A, and ratio B/G are listed in Table 6 using the GGA-PBE approximation. The traditional mechanical stability conditions in cubic crystals are known by the Born and Huang criteria [31]. First of all, it is clear that the conditions satisfy elastic stability, where the bulk modulus B and the three elastic constants (C_{11}, C_{12}, and C_{44}) are all positive [32]. We have shown in this approach that all the compounds studied meet the criteria for mechanical stability according to the following relationships [33]:

$$C_{11}-C_{12} > 0; \quad C_{11} > 0, C_{44} > 0; \quad (C_{11} + 2C_{12}) > 0; \quad C_{12} < B < C_{11}$$

So these two RhFeX (with X = Ge, Sn) materials are mechanically stable. From these elastic constants, other quantities can be deduced, such as the shear modulus G, the Young's modulus E, the Poisson's coefficient υ, and the anisotropy parameter A which can be derived by means of the following relationships [34]:

$$A = \frac{2C_{44}}{(C_{11}-C_{12})} \tag{3}$$

$$B = \frac{1}{3}(C_{11} + 2C_{12}) \tag{4}$$

$$G_v = 1/5(C_{11}-C_{12} + 3C_{44}) \tag{5}$$

$$G_R = \frac{5C_{44}(C_{11}-C_{12})}{4C_{44} + 3(C_{11}-C_{12})} \tag{6}$$

$$G = \frac{G_v + G_R}{2} \tag{7}$$

$$Y = \frac{9BG}{3B + G} \tag{8}$$

$$\upsilon = \frac{(3B-Y)}{6B} \tag{9}$$

For isotropic crystal, the anisotropy parameter A is equal to 1, while another higher or lower value of the unit means that it is an anisotropic crystal. According to Table 6, the values of the anisotropy A parameters obtained are 6.58 and 9.93 for RhFeGe and RhFeSn, respectively. It can be deduced that the calculated values are much larger than 1; this means that these compounds are characterized by deep elastic anisotropy and have a low probability of developing microcracks or structural defects during its growth process. From the point of view of the ductility and brittleness of a material, it is necessary to present two factors: the Pugh ductility index B/G and the Poisson coefficient υ; we started with the interpretation of the ratio B/G where the critical value that separates ductile and fragile behavior is equal to 1.75 (brittle < 1.75 < ductile) [6, 35]. For RhFeX (with X = Ge, Sn) materials, the ratio B/G is equal to 3.02 and 3.11, respectively, that classify these two compounds as ductile materials.

Frantsevich et al. [36] also separated the ductile and brittle behavior of the materials in terms of the Poisson coefficient υ. According to the Frantsevich rule, the critical value is equal to

Table 6 Calculated elastic constants C_{ij} and the bulk modulus B (in GPa), anisotropy factor A, shear modulus G (in GPa), Young's modulus Y (in GPa), and the Poisson's ratio υ of the cubic RhFeGe and RhFeSn

Material	Method	C_{11}	C_{12}	C_{44}	B	A	G	Y	B/G	υ
RhFeGe	GGA (PBE)	172.0	140.7	102.9	151.2	6.58	49.9	134.9	3.02	0.35
RhFeSn		144.3	124.6	98.1	131.2	9.93	42.1	114.1	3.11	0.35

0.26 as a barrier term; if the Poisson coefficient is lower than this value, the material is fragile; beyond this interval, the material will become ductile. For RhFeGe and RhFeSn compounds, the Poisson coefficient υ is 0.35. The calculated υ values are greater than 0.26, which further confirm the ductility of these materials. The value of the Poisson coefficient also makes it possible to provide or know the types of binding in a solid [37], the Poisson coefficient υ for covalent materials is less than 0.1 but for ionic materials, it is greater than or equal to 0.25. The calculated values of Poisson coefficient for both compounds confirm the ionic binding of these materials. The rigidity of any given compound is expressed by the Young's modulus E, and as seen in Table 6, the two materials are more rigid. The longitudinal velocity, the transverse velocity and the mean velocity of the elastic wave propagation, and the Debye temperature are related to the value of the bulk modulus B and the shear modulus G; these quantities can be calculated with the following relationships [38, 39]. The longitudinal and transverse sound velocities (V_l and V_t) are given by the following expressions:

$$V_l = \left(\frac{3B + 4G}{3\rho}\right)^{1/2} \tag{10}$$

$$V_t = \left(\frac{G}{\rho}\right)^{1/2} \tag{11}$$

where ρ is the density.

The average sound velocity V_m is given by the following relationship:

$$V_m = \left[\frac{1}{3}\left(\frac{2}{V_t^3} + \frac{1}{V_l^3}\right)\right]^{-1/3} \tag{12}$$

$$\theta_D = \frac{h}{k_B}\left[\frac{3n}{4\pi} \times \frac{N_A\rho}{M}\right]^{\frac{1}{3}} \times V_m \tag{13}$$

θ_D is the Debye temperature, h is the Planck constant, k_B is the Boltzmann constant, N_A is the Avogadro number, and M is the molecular weight.

The Debye temperature is directly related to the elastic constants through the average propagation rate; any decrease in the value of V_m leads to a decrease in the Debye temperature.

The density ρ, longitudinal sound velocities V_l and transverse sound velocities V_t, mean sound velocity V_m, and Debye temperature θ_D at zero pressure are listed in Table 7 for half-Heusler alloys RhFeX (with X = Ge and Sn) using the GGA approximation. From this table, the values of θ_D are 439.36 K and 377.55 K for RhFeGe and RhFeSn, respectively; we can see that both compounds exhibit high Debye temperatures, which indicate that they have important thermal conductivities.

Table 7 Calculated values of density of mass ρ ($\times 10^3$ in kg m^{-3}), longitudinal (V_l), transverse (V_t) and average sound velocity (V_m in m s^{-1}), and Debye temperature (θ_D in K) for RhFeGe and RhFeSn

Material	ρ	V_l	V_t	V_m	θ_D
RhFeGe	7.887	2516.25	5254.840	3396.70	439.36
RhFeSn	8.293	2253.82	4753.536	3047.75	377.55

3.5 Thermodynamic Properties and Dispersion of Phonon

The calculation of the thermodynamic properties of materials is very important in the field of solid-state physics and industrial applications. In addition, investigating these properties is of great interest to extend our knowledge of their specific behavior when materials are subjected to the effect of high pressure and high environmental temperature. To study the thermodynamic properties of RhFeX (with X = Ge, Sn) alloys, we apply in particular the Debye quasi-harmonic model which is implemented in the Gibbs program [15, 40]. The purpose of this analysis is to determine the evolution of thermodynamic properties as a function of temperature, such as the bulk modulus (B), the constant volume calorific capacity (C_V), the Debye temperature (θ_D), and the thermal expansion coefficient (α). The thermodynamic properties are determined in the temperature range between 0 and 950 K, as well as the pressure effect is imposed in the range 0 to 40 GPa, where the pressure points are taken with a step of 8 GPa using the GGA-PBE approximation.

The bulk modulus represents the material's resistance to volume change when compressed. The evolution of the bulk modulus with temperature and pressure is shown in Fig. 7 (a1, a2) for RhFeGe and RhFeSn compounds. From 0 to 100 K, the bulk modulus is almost constant but beyond 100 K, it decreases. The same trend is noticed for various pressure values. The bulk modulus increases almost linearly with pressure at any given temperature. Thus, compressibility decreases with temperature growth at a given pressure and increases with pressure at a given temperature. In conclusion, the hardness of these two materials RhFeGe and RhFeSn decreases with increasing temperature and increases when compressed. The calculations of bulk modulus B at zero pressure and zero temperature are 148.5 GPa and 128.2 GPa for RhFeGe and RhFeSn, respectively, indicating that these values are in good agreement with those obtained from structural properties (see Table 2) as well as those calculated by elastic constants (see Table 6).

The specific heat of a material is another important thermodynamic property that is mainly due to the vibrating

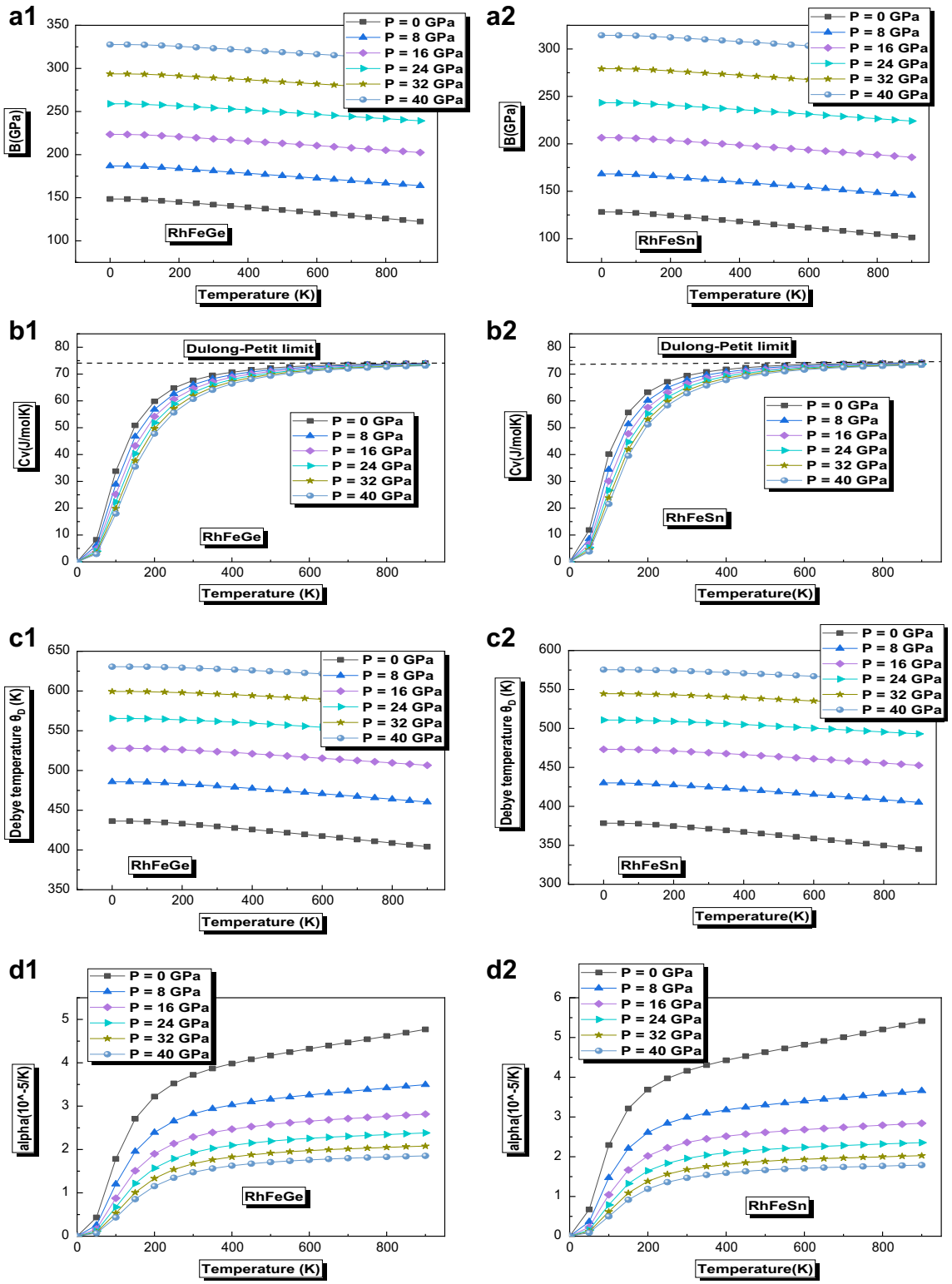

Fig. 7 The variation as a function of temperature for RhFeGe and RhFeSn at different pressures of (a1, a2) the Bulk modulus B, (b1, b2) the heat capacity C*v*, (c1, c2) the Debye temperature θ_D, and (d1, d2) the thermal expansion coefficient

movement of ions. The movement of free electrons corresponds to a small part of the heat that becomes important at high temperatures, especially in transition metals that have incomplete electron layers. The thermal capacity of a substance is a measure of how much heat is stored. Every time when heat is supplied to a material, this will necessarily lead to an increase in temperature; hence, its calorific capacity gives an indication for predicting the vibration properties that are

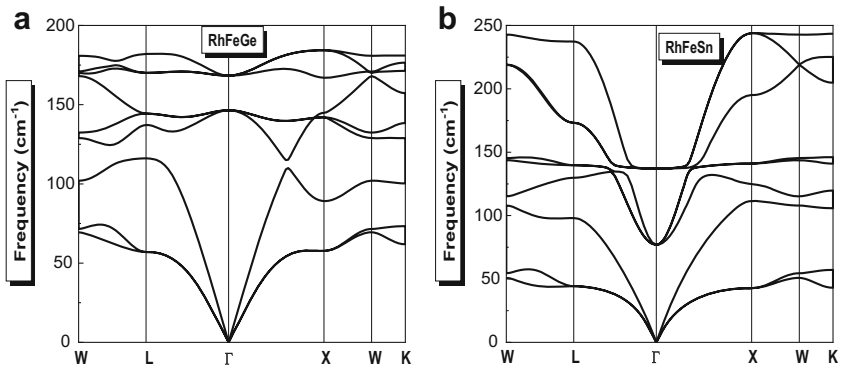

Fig. 8 The calculated phonon dispersion curves of **a** RhFeGe and **b** RhFeSn compounds

required for many applications. As shown in Fig. 7 (b1, b2), the specific heat (C_V) maintains the same temperature-dependent behavior for the two studied compounds. The evolution of the heating capacity at constant volume C_V with temperature at different pressures for RhFeGe and RhFeSn alloys is shown in Fig. 7 (b1, b2). The temperature increase causes a rapid increase in the value of the heating capacity at low temperatures (below 300 K), and then it increases slowly at high temperatures approaching the Dulong and Petit limit [41] which is 74.633 J K^{-1} mol^{-1} and 73.406 J K^{-1} mol^{-1} for RhFeGe and RhFeSn, respectively. This behavior is attributed to all solids at high temperature solids [42]. It can also be seen that at a given temperature, the calorific capacity C_V decreases almost linearly with the increase in the applied pressure.

The Debye temperature θ_D is characteristic of the thermal capacity behavior of solids. It is defined as the maximum temperature that can cause normal vibration of the atoms. Debye's temperature θ_D maintains the same behavior as a function of temperature for the two compounds as shown in Fig. 7 (c1, c2), where it is nearly constant from 0 to 100 K and then decreases almost linearly at temperature values above 100 K. Figure 7 (c1, c2) shows also that at fixed temperature values, θ_D increases linearly with the pressure applied, which makes θ_D behavior towards temperature and pressure quite similar to that of the bulk modulus B. This result is in good agreement with the fact that Debye's temperature is proportional to the bulk modulus and so that a hard material exhibits a high Debye's temperature. Debye temperature θ_D calculations at zero pressure and zero temperature are 436.36 K and 378.45 K for RHFeGe and RhFeSn, respectively, indicating that these values are in good agreement with those calculated from the elastic properties.

The thermal expansion coefficient α define a correlation between the volume of the material and its temperature. The variation of the thermal expansion coefficient α as a function of temperature at various pressures is shown in Fig. 7 (d1, d2) for RhFeGe and RhFeSn, respectively; it can be observed that α first increases with a temperature up to 300 K and then becomes almost constant, while the pressure variation shows the opposite effect namely α decreases with increasing temperature due to lattice compression. However, at fixed temperature, the thermal expansion decreases almost linearly with the increase in pressure and becomes very low at higher temperatures and pressures as well. Thermal expansion coefficient α at 300 K and zero pressure is 3.72×10^{-5} K^{-1} and 4.16×10^{-5} K^{-1} for RHFeGe and RhFeSn, respectively. In order to study the dynamic stability of our compounds, we have calculated the phonon dispersion curves of RhFeGe and RhFeSn. The phonon dispersion calculations were performed by means of the Quantum ESPRESSO package [43] using a plane-wave basis set and ultrasoft pseudo-potentials available in the software. The generalized gradient correction to exchange-correlation potential of Perdew-Burke-Ernzerhof (PBE) was used. Figure 8 shows the calculated phonon dispersion curves of RhFeGe and RhFeSn compounds along high-symmetry directions in Brillouin zone. As expected for Heusler structure with three atoms in the primitive cell, the phonon dispersion curve exhibits nine branches: three acoustic and six optical branches. At zero pressure, our calculations reveal that all phonon modes exhibit positive frequencies, suggesting that RhFeGe and RhFeSn compounds are dynamically stable.

Table 8 Calculated values of electrical conductivity (σ/τ in $10^{20}/\Omega^{-1}$ m^{-1} s^{-1}), electronic thermal conductivity ($\kappa e/\tau$ in 10^{16} W (K m s)$^{-1}$), Seebeck coefficient (S in μV K^{-1}), and figure of merit ZT at 300 K for RhFeGe and RhFeSn in both spin configurations

Materials	Spin state	σ/τ	S	κ_e/τ	ZT
RhFeGe	Up	8.99	− 5.48	0.661	0.001
	Down	3.11×10^{-3}	− 572.60	0.033×10^{-3}	0.934
RhFeSn	Up	8.87	− 6.01	0.652	0.001
	Down	0.05×10^{-3}	841.08	0.012×10^{-3}	0.952

3.6 Thermoelectric Properties

A great deal of interest in thermoelectric materials has grown worldwide due to their aptitude to convert thermal energy into useful energy and reciprocally [44, 45]. The efficiency of these materials finds a huge demand for thermoelectrics through their energy production, dielectrics, and refrigeration

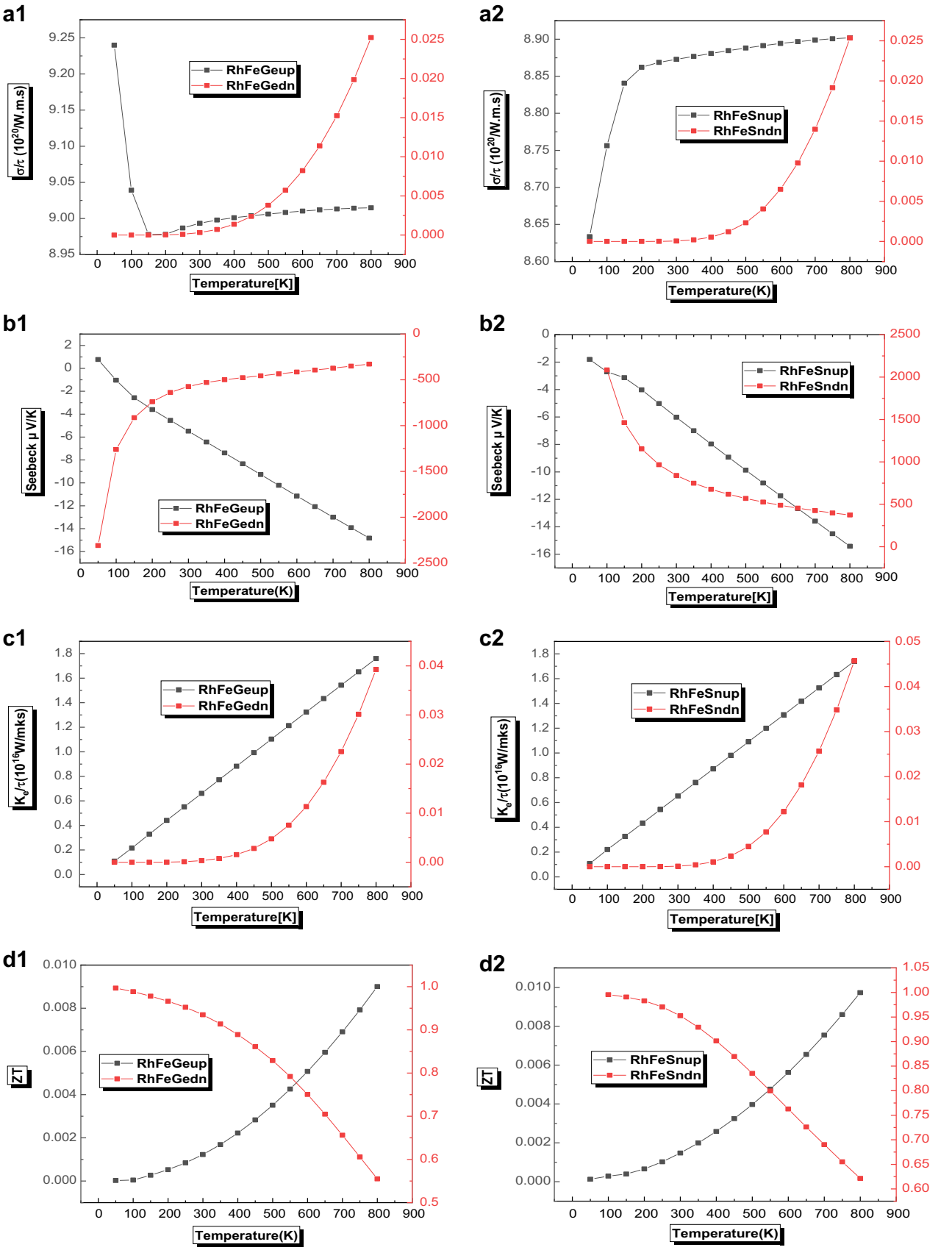

Fig. 9 The variation as a function of temperature for RhFeGe and RhFeSn of (a1, a2) the electrical conductivity (σ/τ), (b1, b2) the Seebeck coefficient (S), (c1, c2) electronic thermal conductivity ($\kappa e/\tau$), and (d1, d2) the Merit factor ZT

capabilities. The transport properties of the two compounds were calculated using the BoltzTraP code [17] under the approximation of the constant relaxation time for charge carriers. This part is devoted to study different transport coefficients of our two RhFeX (with X = Ge, Sn) compounds in both spin states up and down, such as electrical conductivity (σ/τ), electronic thermal conductivity ($\kappa e/\tau$), and Seebeck coefficient (S) as well as the merit factor (ZT). The variation of the electrical conductivity as a function of temperature is shown in Fig. 9 (a1, a2) for RhFeGe and RhFeSn, respectively. For both half-Heusler alloys, the electrical conductivity calculated for the spin up state differs from that found for the spin down state. As to RhFeGe alloy and for the spin up state, there is an unexpected decrease in electrical conductivity with temperature in the range $50 < T < 150$ K and then becomes stable between 150 and 200 K. However, above 200 K, the electrical conductivity slowly increases with increasing temperature and becomes approximately constant. Although a sudden increase in electrical conductivity with temperature in the range $50 < T < 200$ K is seen for the RhFeSn alloy, then above 200 K, the electrical conductivity slowly increases with increasing temperature and attains almost constant value. The spin down state of the two RhFeGe and RhFeSn alloys is identical and varies only very slightly with temperature in the range $50 < T < 400$ K, while at temperatures above 400 K, there is a sudden increase in electrical conductivity. The electrical conductivity values obtained at 300 K for the spin up and spin down states of both compounds RhFeX (with X = Ge, Sn) are shown in Table 8. Figure 9 (b1, b2) shows the evolution of Seebeck coefficient as a function of temperature. Half-Heusler alloys RhFeX (with X = Ge, Sn) reveal a half-metallic behavior. For the spin up state, we can see that for RhFeGe, the found value of Seebeck coefficient is positive up to a temperature of 100 K; then, it becomes negative, while for RhFeSn, this value is negative in the whole temperature range. For the spin down state, we also notice that for the RhFeGe alloy, the increase temperature gives rise to a rapid increase of Seebeck coefficient up to 300 K; then, it increases slowly, whereas for the RhFeSn, there is a rapid decrease of this coefficient up to 300 K and then it decreases slowly. Therefore, for the spin down state, it keeps the same negative sign for the Seebeck coefficient value. For the spin up and spin down states, the Seebeck coefficient values around the ambient temperature (300 K) are illustrated in Table 8 for both half-Heusler alloys RhFeGe and RhFeSn. The negative sign of the Seebeck coefficient observed for RhFeGe and RhFeSn suggests that the conduction was made by negative charge carriers (electrons); thus, these materials are of type n. The variation of the electronic thermal conductivity κ_e/τ as a function of temperature of the RhFeX (with X = Ge, Sn) for both spin up and spin down states is shown in Fig. 9 (c1, c2). As it can be seen, for the spin up state, the electronic thermal conductivity increases linearly with the temperature for both alloys RhFeGe and RhFeSn. The κ_e/τ values at 300 K correspond to about 6.61×10^{15} and 6.52×10^{15} W m^{-1} K^{-1} s^{-1} for RhFeGe and RhFeSn compounds, respectively. While for the spin down state, the electronic thermal conductivity also increases with temperature but not linearly as for the spin up state. The κ_e/τ values around the ambient temperature (300 K) are 3.30×10^{12} and 1.20×10^{12} W m^{-1} K^{-1} s^{-1} for RhFeGe and RhFeSn, respectively. The electronic thermal conductivities for the spin up and spin down states are shown in Table 8 for RhFeGe and RhFeSn alloys, respectively.

In order to quantify the thermoelectric efficiency of these compounds, we have calculated the variation of the figure of merit over a temperature range from 50 to 800 K. The figure of merit (ZT) for both spin up and spin down states is shown in Fig. 9 (d1, d2). For the spin up state, the value of ZT increases with temperature for both compounds. The value of ZT values at $T = 300$ K is 0.001 for these alloys. These values are really low mainly because of their large thermal electronic conductivities and should be even smaller if the lattice thermal conductivity is taken into account. While for the spin down state, the value of ZT decreases with increasing temperature, the values of ZT at 300 K are 0.935 and 0.952 for RhFeGe and RhFeSn materials, respectively (see Table 8), which confirm that these two materials are potentially good candidates for thermoelectric applications at low temperature.

4 Conclusion

In this work, using full potential linearized augmented plane wave FP-LAPW method, we have thoroughly studied the structural, elastic, electronic, magnetic, thermodynamic, and thermoelectric properties of the RhFeGe and RhFeSn half-Heusler alloys due to their technological and industrial interests. The results and conclusions of this work can be summarized as follows:

- The study of structural properties reveals that RhFeX with (X = Ge, Sn) alloys have lattice parameters close to other calculations. The negative values of formation energy ΔH_f and cohesive energy E_{coh} found for both compounds indicate that these materials are thermodynamically stable and could be experimentally synthesized.
- From the study of the electronic properties, we show that the compounds RhFeGe and RhFeSn have a half-metallic (HFM) behavior with indirect band gap using both GGA-PBE and mBJ-GGA approximations.
- The total magnetic moment (μ_{tot}) per cell unit is an integer value of 3 μB for both compounds, which confirm the half-metallic nature of these two compounds. This value is in line the Slater Pauling rule: $\mu_{\mathrm{tot}} = (Z_{\mathrm{tot}} - 18)$.
- The obtained results from the elastic properties show that both compounds are mechanically stable and are

classified as ductile materials. The thermodynamic properties including the isothermal bulk modulus, the heat capacity, the Debye temperature, and the thermal expansion coefficients of these compounds are investigated using the quasi-harmonic Debye model in the temperature range of 0–950 K and pressure range of 0–40 GPa. The observed variations accord well with the results of the Debye theory, which is regularly applied to several materials. The study of phonon dispersion reveals that both materials are dynamically stable.

– Finally, the effects of temperature on thermoelectric parameters are investigated using BoltzTraP code. RhFeGe and RhFeSn ternary half-Heuslers which have a high thermoelectric power (− 572.60 μV K^{-1} and 841.08 μV K^{-1}), a high electrical conductivity (3.11×10^{16} $(\Omega\ m\ s)^{-1}$ and 5×10^{15} $(\Omega\ m\ s)^{-1}$), and low electronic thermal conductivity (3.3×10^{12} W $(K\ m\ s)^{-1}$ and 1.2×10^{12} W $(K\ m\ s)^{-1}$, respectively), which give them a high figure of merit ZT coefficient of 0.935 and 0.952 at room temperature. Thus, these half-Heusler alloys are good candidates for thermoelectric device applications at low temperature.

References

1. Groot, R.A., Mueller, F.M., van Engen, P.G., Buschow, K.H.J.: Phys. Rev. Lett. **50**, 2024–2027 (1983)
2. Murnaghan, F.D.: Proc. Natl. Acad. Sci. U. S. A. **30**, 244–247 (1947)
3. Xiong, L., Yi, L., Gao, G.Y.: J. Magn. Magn. Mater. **360**, 98–103 (2014)
4. Hohenberg, P., Kohn, W.: Phys. Rev. **136**, 864–871 (1964)
5. Kohn, W., Sham, L.J.: Phys. Rev. **A 140**, 1133–1138 (1965)
6. Perdew, J.P., Chevary, J.A., Vosko, S.H., Jackson, K.A., Pederson, M.R., Singh, D.J., Fiolhais, C.: Phys. Rev. **B 46**, 6671–6687 (1992)
7. Slater, J.C.: Adv. Quantum Chem. **1**, 55–64 (1964)
8. Perdew, J.P., Burke, K., Ernzerhof, M.: Phys. Rev. Lett. **77**, 3865–3868 (1996)
9. Perdew, J.P., Wang, Y.: Phys. Rev. **B45**, 13 244–13 249 (1992)
10. Otero-de-la Roza, A., Luaña, V.: Comput. Phys. Commun. **180**, 800–812 (2009)
11. Rogl, G., Grytsiv, A., Gürth, M., Tavassoli, A., Ebner, C., Wünschek, A., Puchegger, S., Soprunyuk, V., Schranz, W., Bauer, E., Müller, H., Zehetbauer, M., Rogl, P.: Acta Mater. **107**, 178 (2016)
12. Blaha, P., Schwarz, K., Madsen, G. K. H., Kvasnicka, D., Luitz, J.: "WIEN2k, an augmented plane wave plus local orbitals program for calculating crystal properties," 2th Edition, Vienna University of Technology, Vienna (2001).
13. Tran, F., Blaha, P.: Accurate band gaps of semiconductors and insulators with a semilocal exchange-correlation potential. Phys. Rev. Lett. **102**, 226401–226404 (2009)
14. Blaha, P., Schwarz, K., Madsen, G.K.H., Hvasnicka, D., Luitz, J.: Wien2k: an Augmented Plane Wave plus Local Orbitals Program for Calculating Crystal Properties. Vienna University of Technology, Austria (2001)
15. Blanco, M.A., Francisco, E., Luaña, V.: Comput. Phys. Commun. **158**, 57–72 (2004)
16. Songke, F., Shuangming, L., Hengzhi, F.: Comput. Mater. Sci. **82**, 45 (2014)
17. Madsen, G.K., Singh, D.J., Boltztrap: Comput. Phys. Commun. **175**(1), 67–71 (2006)
18. Bulusu, A., Walker, D.G.: Review of electronic transport models for thermoelectric materials. Superlattice. Microst. **44**, 1–36 (2008)
19. Feng, L., Liu, E., Zhang, W., Wang, W., Wu, G.: First-principles investigation of half-metallic ferromagnetism of half-Heusler compounds XYZ. J. Magn. Magn. Mater. **351**, 92–97 (2014)
20. Webster, P.J., Ziebeck, K.R.A.: Landolt-Börnstein - group III condensed matter, vol. 19C, pp. 75–184. Springer, Berlin (1988)
21. Murnaghan, F.D.: Proc. Natl. Acad. Sci. **30**, 244 (1944)
22. Ma, J., Hegde, V.I., Munira, K., Xie, Y., Keshavarz, S., Mildebrath, D.T., Wolverton, C., Ghosh, A.W., Butler, W.H.: Computational investigation of half-Heusler compounds for spintronics applications. Phys. Rev. B. **95**, 024411 (2017)
23. Johnson, K.A., Ashcroft, N.W.: Phys. Rev. **B 58**, 15548 (1998)
24. Kacimi, S., Mehnane, H., Zaoui, A.: J. Alloys Compd. **587**, 451 (2014)
25. Yadav, M.K., Sanyal, B.: First principles study of thermoelectric properties of Li-based half-Heusler alloys. J. Alloys Compd. **622**, 388–393 (2015)
26. Chibani, S., Arbouche, O., Zemouli, M., Amara, K., Benallou, Y., Azzaz, Y., Ameri, M.: J. Electron. Mater. **47**(1), 196 (2017)
27. Haque, E., Hossain, M.A.: Results Phys. **10**, 458 (2018)
28. Yao, K.L., Gao, G.Y., Liu, Z.L., Zhu, L.: Solid State Commun. **133**, 301 (2005)
29. Gao, G.Y., Yao, K.L., Sasioglu, E., Sandratskii, L.M., Liu, Z.L., Jiang, J.L.: Phys. Rev. **B 75**, 174442 (2007)
30. Galanakis, T., Endo, K., Chieda, Y., Sugawara, T., Obara, K., Shishido, T., Matsubayashi, K.Y., Uwatoko, H., Nishihara, R., Umetsu, Y., Nagasako, M., Kainuma, R.: J. Alloys Compd. **505**, 29 (2010)
31. Born, M., Huang, K.: Dynamical Theory and Experiment I, ed, pp. 1–415. Springer Verlag, Berlin (1982)
32. Wallace, D.C.: Thermodynamics of Crystals, ed, pp. 1–484. Dover Publications, INC, Wiley, Mileona (1972)
33. Nye, J.F.: Physical Properties of Crystals. Oxford University Press, Oxford (1985)
34. Hill, R.: Proc. Phys. Soc. Lond. **A 65**, 349 (1952)
35. Nye, J.F.: Physical Properties of Crystals. Clarendon, Oxford (1957)
36. Frantsevich, I.N., Voronov, F.F., Bakuta, S.A.: In: Frantsevich, I.N. (ed.) Naukova Dumka, Kiev, 1983Elastic Constants and Elastic Moduli of Metals and Insulators Handbook, pp. 60–180. NaukovaDumka, Kiev (1982)
37. Haines, J., Leger, J.M., Bocquillon, G.: Annu. Rev. Mater. Sci. **31**, 1 (2001)
38. E. Schreiber and O. L. Anderson, N. Soga, Elastic Constants and Their Measurements (book) 1973, pp 82–125
39. Wachter, P., Filzmoser, M., Rebizant, J.: Phys. B Condens. Matter. B293,223 (2001)
40. Otero-de-la-Roza, A., Abbasi-Pérez, D., Luana, V.: Comput. Phys.Commun. **182**, 2232 (2011)
41. Petit, A.T., Dulong, P.L.: Ann. Chim. Phys. **10**, 395 (1819)
42. Giannozzi, P., et al.: QUANTUM ESPRESSO: a modular and open-source software project for quantum simulations of materials. J. Phys. Condens. Matter. **21**, (2009)
43. Chang, J., Chen, X.R., Zhang, W., Zhu, J.: Chin. Phys. **B 17**, 1377 (2008)
44. Tan, X.J., Liu, W., Liu, H.J., Shi, J., Tang, X.F., Uher, C.: Phys. Rev. B. **85**, 205 (2012)
45. Pei, Y., Wang, H., Snyder, G.J.: Adv. Mater. **24**, 6125 (2012)